Amorphous HfO_2 and $Hf_{1-x}Si_xO$ via a melt-and-quench scheme using *ab initio* molecular dynamics

Wanderlã L. Scopel,[1,*] Antônio J. R. da Silva,[2] and A. Fazzio[2,3]

[1]*Departamento de Ciências Exatas, Pólo Universitário de Volta Redonda, Universidade Federal Fluminense, Av. dosTrabalhadores, 420, CEP 27255-250, Volta Redonda, RJ, Brazil*

[2]*Instituto de Física, Universidade de São Paulo, Caixa Postal 66318, CEP 05315-970 São Paulo, SP, Brazil*

[3]*Centro de Ciências Naturais e Humanas, Universidade Federal do ABC, Santo André, SP, Brazil*

(Received 27 October 2007; revised manuscript received 26 March 2008; published 6 May 2008)

We have performed *ab initio* molecular dynamics simulations to generate an atomic structure model of amorphous hafnium oxide (a-HfO_2) via a melt-and-quench scheme. This structure is analyzed via bond-angle and partial pair distribution functions. These results give a Hf-O average nearest-neighbor distance of 2.2 Å, which should be compared to the bulk value, which ranges from 1.96 to 2.54 Å. We have also investigated the neutral O vacancy and a substitutional Si impurity for various sites, as well as the amorphous phase of $Hf_{1-x}Si_xO_2$ for x=0.25, 0.375, and 0.5.

DOI: 10.1103/PhysRevB.77.172101 PACS number(s): 61.72.J−, 71.55.Ht, 71.15.Mb

Among all of the high-dielectric-constant materials (high-k materials) that have been considered as possible replacements for SiO_2 as a gate dielectric, hafnium oxide (HfO_2) and its silicate ($HfSi_xO_y$) stand out as two of the most promising ones.[1] Two key properties are responsible for this interest, viz., their much higher dielectric constants when compared to that of SiO_2 (~20 versus 3.9 for SiO_2) and their thermodynamic stability when in contact with Si. Moreover, interfacial properties,[2] such as the presence of defects and interface states, are fundamental for their use in the metal oxide semiconductor technology.

The usual growth of the HfO_2 dielectric leads to an amorphous phase, which upon further thermal processing tends to recrystallize. Defects in the HfO_2 crystalline bulk can be quite detrimental to the behavior of the devices since they can lead to flatband voltage instabilities.[3,4] It is believed that the oxygen vacancy is the relevant defect in HfO_2 related to these reliability problem.[5,6]

Many experimental works[7–9] explored various techniques and experimental conditions for growth processing and annealing of a stable amorphous phase of these high-k materials. From a theoretical side, there are just a few studies of the amorphous phase of HfO_2.[10–12] However, besides the study of the intrinsic amorphous phase, it is relevant to investigate the properties of defects. In particular, as stated above, the presence of oxygen vacancies may be quite deleterious for the device behavior. Since these vacancies may be created before the recrystallization phase, it is important to understand how their formation energies, and properties in general, vary in the amorphous phase. Moreover, since the trend is to use not HfO_2 but rather a $Hf_{1-x}Si_xO_2$ silicate, it is also important to study a substitutional Si impurity (Si_{Hf}—limit of very small x) as well as the amorphous phase of $Hf_{1-x}Si_xO_2$ for different values of x.

In the present work, we address the a-HfO_2 atomic structure generated via *ab initio* molecular dynamics simulations (AIMD),[13] based on the density functional theory (DFT). By using this generated model as a prototype for the a-HfO_2, we have investigated its structural and electronic properties, as well as the characteristics of oxygen vacancies. We have also studied substitutional Si_{Hf} in the a-HfO_2, as well as three amorphous structures of $Hf_{1-x}Si_xO_2$ for x=0.25, x=0.375, and x=0.5.

The relaxed monoclinic structure (m-HfO_2) has two nonequivalent oxygen sites, which are threefold and fourfold coordinated. All Hf atoms are equivalent and are sevenfold coordinated. All of these will change in the amorphous phase. From both the crystalline and the amorphous optimized structures, we have performed short simulations of 50 MD steps, for an average temperature of 300 K, in order to calculate the partial pair-radial distribution functions $g_{\alpha,\beta}(r)$ (RDFs), for α,β=Hf, O, which are shown in Fig. 1. For the crystal Hf-Hf pair-distribution function, there are many peaks within the range of 3.30–4.00 Å, which results in a rather broad first peak at 3.40±0.50 Å in the amorphous pair-distribution function.

From the Hf-O pair-distribution functions in the crystal, it is possible to see that there are four types of Hf-O first-nearest-neighbors, with bond distances within the range of 2.03–2.25 Å. In the amorphous structure, the first peak in the Hf-O RDF is at 2.20±0.30 Å. The peak center compares well to the average Hf-O bond length in the crystalline phase of 2.14 Å; however, the peak width becomes almost three times broader, ≃0.6 Å, than the spread of bond lengths in the crystal, ≃0.22 Å. This seems to be a little broader than what was recently obtained for amorphous structures of ZrO_2,[17] but is similar to another simulation of the amorphous HfO_2.[12] Even though recent experimental measurements[18] agree with our Hf-O peak position, the width has not been determined, and further experimental measurements are needed in order to verify if this difference between ZrO_2 and HfO_2 is an intrinsic feature of these systems or is due to variations in the procedures employed to generate the amorphous structure. Finally, for the O-O RDF in the crystal, there are various peaks between 2.50–3.00 Å and one single peak at approximately 3.50 Å. In the amorphous structure, once more these peaks result in a very broad first peak at 2.75±0.50 Å, with a total width of ≃1.0 Å.

The coordination number of each atom is determined by counting the number of atoms within a cutoff radius of 2.50 Å, which has been established from the behavior of the first peak in the Hf-O RDF. In Figs. 2(a) and 2(b), we present

 ©2008 The American Physical Society

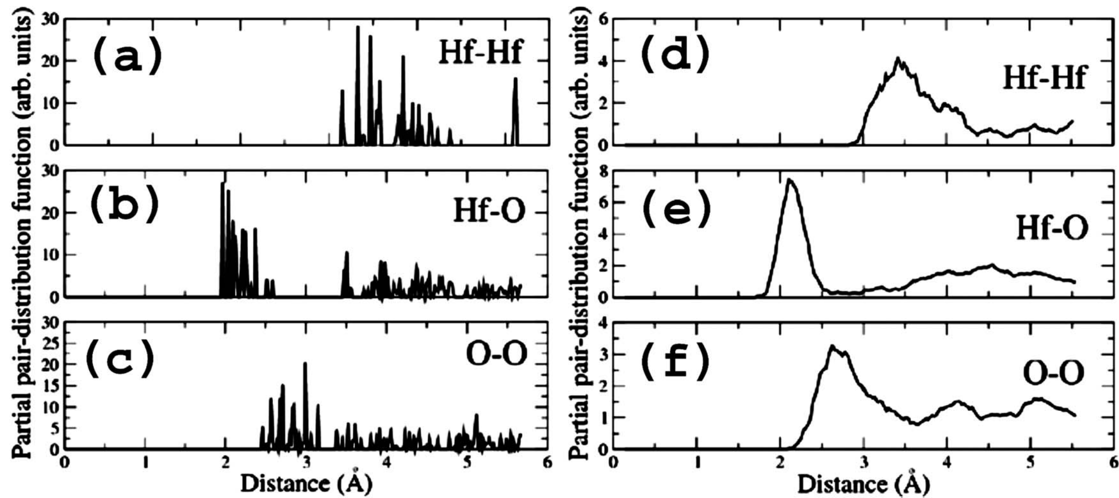

FIG. 1. Partial pair-distribution functions for (left panel) m-HfO_2 and (right panel) a-HfO_2.

the histogram of coordination number for the O and Hf atoms in our m-HfO_2 supercell, respectively. Similar graphs are shown in Figs. 2(c) and 2(d) and Figs. 2(e) and 2(f) for the liquid ($T=5500$ K) and amorphous phases, respectively. In the m-HfO_2, 50% of O atoms have a coordination number equal to three and 50% have a coordination number equal to four. Upon melting, there is a significant increase of the three-coordinated O atoms and the appearance of some two-coordinated oxygen. This is similar but slightly distinct from another theoretical result[10] that obtained a larger number of three coordinated, and consequently, a smaller number of four coordinated O atoms. However, this difference does not seem to affect in an essential way the overall electronic properties, as will be discussed.

In the DFT calculations, for the a-HfO_2 and m-HfO_2 we have found band-gap energies of 3.4 and 3.8 eV, respectively. The latter value is underestimated by about 33%, as compared to the experimentally measured value of 5.68 eV,[19] but is in good agreement with previous DFT calculations.[20] Very similar results were obtained by other theoretical calculations,[10,11] which indicates, as mentioned above, that the overall electronic structure is not very sensitive to the structural details, such as the precise distribution of Hf coordination number.

We considered the formation of neutral oxygen vacancies (V_O), in a-HfO_2, since they can be created in films and bulk samples due to the growth cycle. The neutral oxygen vacancy in the a-HfO_2 was generated by simple removal of an oxygen atom, followed by full relaxation of all remaining atoms. The formation energies for a V_O in HfO_2, $E_f(V_O)$, were calculated as $E_f^{HfO_2}(V_O)=[E_t^{HfO_2}(V_O)+\mu_O]-[E_t(HfO_2)]$, where $E_t^{HfO_2}(V_O)$ and $E_t(HfO_2)$ are the total energies of supercells of amorphous HfO_2 with and without an oxygen vacancy, respectively. The oxygen chemical potential μ_O was considered as the total energy of an isolated oxygen atom in the triplet ground state.[11]

As mentioned above, the monoclinic phase has two kinds of nonequivalent oxygen atoms. In this way, we have determined the formation energy for both vacancy types, and we obtain a formation energy difference of around 0.02 eV. In the amorphous HfO_2, the neutral oxygen vacancy was created at various sites of the structure, and we obtained a formation energy that varies from 8.43 up to 9.52 eV and a formation energy difference of around 1.09 eV (see Table I). It is important to point out that the formation energy of the neutral oxygen vacancy in the monoclinic HfO_2 is 9.32 eV.[21] Therefore, there are vacancies with formation energies that are almost 1 eV smaller than in the crystal, indicating that it might even be easier to create them in the amorphous phase. This is also supported by the fact that the average value of the formation energy obtained from the nine studied vacancies is 8.79 eV, which is also smaller than the bulk value. This is similar to what was obtained by Broqvist and Pasquarello,[11] which was an average value of 8.85 eV. Even though it was argued that the smaller coordination number in the amorphous phase is the cause for this reduction in the formation energy value,[12] we find some cases wherein a vacancy created in a site with coordination number two has a larger formation energy than sites with higher coordination numbers (see Table I). It is also important to point out that

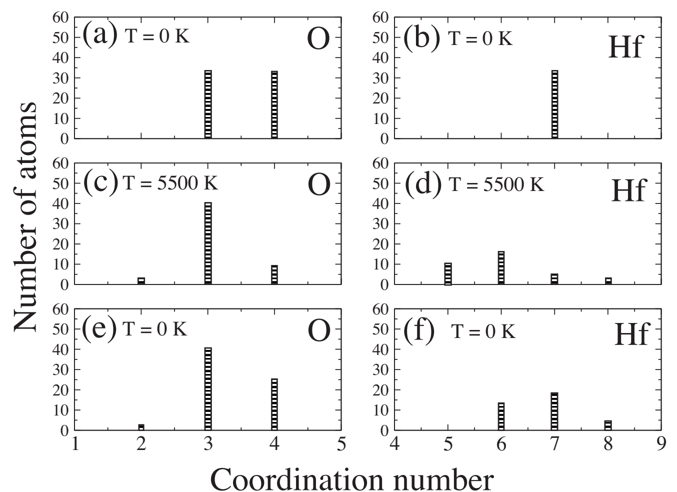

FIG. 2. Distribution of coordination numbers in the monoclinic [(a) and (b)], liquid [(c) and (d)], and amorphous [(e) and (f)] phases, for the oxygen and hafnium atoms.

TABLE I. Distances between the oxygen atoms where the vacancies will be created (labeled V1–V9) and their Hf nearest neighbor atoms (in Å). The coordination number N_V and the formation energy E_f for each vacancy are also presented (eV). In the last column, we present the position of the doubly occupied vacancy level in the gap relative to the top of the valence band in the amorphous phase (eV).

Label	d_1	d_2	d_3	d_4	N_V	E_f	ε_{vac}
V_1(a)	1.95	1.99	2.14		3	8.43	2.40
V_2(a)	2.01	2.05	2.17		3	8.49	1.95
V_3(a)	2.06	2.08	2.19	2.48	4	8.51	2.36
V_4(a)	2.11	2.13	2.14	2.27	4	8.52	2.28
V_5(a)	2.04	2.09	2.14		3	8.73	2.46
V_6(a)	1.99	2.05			2	8.82	2.53
V_7(a)	2.14	2.16	2.17	2.45	4	8.96	2.16
V_8(a)	2.11	2.19	2.31	2.31	4	9.03	2.02
V_9(a)	2.09	2.16	2.24	2.46	4	9.52	1.61

calculations showed that[21] an oxygen vacancy in crystalline SiO_2 is more stable than in HfO_2 by approximately 1.2 eV, implying that if a crystalline HfO_2 is grown on top of a Si substrate and there is also a SiO_2-like interfacial layer, it will be easier to create vacancies in it as compared to in the bulk hafnia. However, as in the amorphous HfO_2 there are vacancies with formation energies close to 1 eV lower than in the crystalline phase, this tendency of creating oxygen vacancies in the silica layer and at the same time healing oxygen vacancies in the HfO_2 is weakened.

In the monoclinic phase, the formation of a neutral oxygen vacancy introduces a new state in the band gaps situated at 2.8 and 2.3 eV above the top of the valence band[22] for threefold and fourfold coordinated oxygen, respectively. In the amorphous structure, the formation of neutral oxygen vacancies introduce new states in the band gap within the range between 1.61 and 2.53 eV above the top of the valence band of the amorphous phase, with an average value of 2.19 eV. Thus, in general, the levels will be closer to the top of the valence band than in the crystalline phase. Moreover, there is no general trend that correlates either the value of the formation energy or the coordination number to the position of the level.

Due to the interest in the silicate phase[23] $Hf_{1-x}Si_xO_2$, we have investigated (1) substitutional Si atoms, which would be the limit of very small x and (2) three amorphous structures of $Hf_{1-x}Si_xO_2$ for $x=0.25$, $x=0.375$, and $x=0.5$. These latter structures were generated in the following way: from the HfO_2 liquid phase at 5500 K, we have substituted a given number of Hf atoms by Si, and then we quenched the system as described before in the generation of the amorphous structure of HfO_2.

TABLE II. Distances between the Si atom and the O nearest neighbor atoms (in Å).

Label	d_1	d_2	d_3	d_4	d_5
Si_{Hf}^1	1.62	1.64	1.65	1.68	
Si_{Hf}^2	1.64	1.65	1.68	1.69	
Si_{Hf}^3	1.60	1.66	1.68	1.70	
Si_{Hf}^4	1.63	1.64	1.67	1.69	
Si_{Hf}^5	1.72	1.75	1.77	1.79	1.83

TABLE III. Fraction of Si with a given coordination of O atoms (for a cutoff of 2.0 Å). In the parentheses are the average Si-O distances (in Å), for the three $Hf_{1-x}Si_xO_2$ structures.

$Hf_{1-x}Si_xO_2$	Number of first nearest-neighbors		
x	4	5	6
0.250	0.625(1.63)	0.250(1.76)	0.125(1.83)
0.375	0.917(1.64)	0.083(1.74)	
0.500	0.875(1.64)	0.125(1.74)	

For the substitutional Si, we have studied five distinct Hf sites, which were obtained from the final structure of a-HfO_2 by replacing Hf atoms by Si ones and then relaxing the forces. Thus, no annealing was performed in these cases. It is interesting to note that in four of the final relaxed structures the Si atoms became fourfold coordinated, even though the Hf atom had initially six nearest neighbors. In the other structure, the Si was fivefold coordinated, similar to what was observed[24] before in Si-rich $Hf_{1-x}Si_xO_2$ structures, albeit these latter systems were not amorphous. All of the final Si-O distances in the fourfold coordinated Si are within the range of 1.60–1.70 Å, whereas in the fivefold coordinated case they are within the range of 1.72–1.83 Å, as can be seen in Table II.

In Tables III and IV, we present an analysis of the coordination numbers of Si and Hf, respectively, for the three $Hf_{1-x}Si_xO_2$ amorphous structures. We have not observed any tendency of phase separation during the quenching, even though most likely it was too fast to be able to allow the necessary atomic migration. Most of the Si atoms end up tetracoordinated, but in all cases we have a significant fraction of pentacoordinated atoms. For $x=0.25$, we have even observed one Si atom that had six oxygen neighbors, even though one of the Si-O distances was quite large (1.98 Å). As the concentration x increases, the number of tetracoordinated Si atoms increases. The average Si-O distances in this case remains close to 1.6 Å, similar to in SiO_2. This is smaller than what is obtained for crystalline $Hf_{1-x}Si_xO_2$ for similar concentrations,[25] indicating that in the amorphous

TABLE IV. Fraction of Hf with a given coordination of O atoms (for a cutoff of 2.8 Å). In the parentheses are the average Hf-O distances (in Å), for the three $Hf_{1-x}Si_xO_2$ structures.

$Hf_{1-x}Si_xO_2$	Number of first nearest-neighbors			
x	5	6	7	8
0.250	0.125(2.11)	0.250(2.11)	0.417(2.17)	0.208(2.22)
0.375	0.100(2.05)	0.500(2.10)	0.400(2.17)	
0.500	0.353(2.06)	0.353(2.11)	0.176(2.19)	0.118(2.22)

phase, these Si-O distances are better accommodated. In the case of pentacoordinated Si, the average Si-O distances are larger, between 1.7 and 1.8 Å.

For Hf atoms we observe that as x increases, there is a tendency to decrease the average coordination. As opposed to in a-HfO_2, in the $Hf_{1-x}Si_xO_2$ structures we observe pentacoordinated Hf atoms, which increase in number as the content of Si increases. In the a-HfO_2, the majority of Hf atoms have a coordination number of seven. However, in the $Hf_{1-x}Si_xO_2$ structures this happens only for $x=0.25$, and there is a shift toward hexa- and pentacoordinated Hf atoms as x increases. The average Hf-O distances for both penta- and hexacoordinated Hf atoms are 2.1 Å, whereas for hepta- and octacoordinated this average distances are closer to 2.2 Å. Even though these results were obtained for only three particular quenching ramps, we expect the trends to be valid in general.

In summary, we have generated a model of amorphous structures of HfO_2 and $Hf_{1-x}Si_xO_2$ for $x=0.25$, 0.375, and 0.5 via a melt-and-quench scheme using AIMD calculations. We have investigated oxygen vacancies in a-HfO_2, and we have found that there is an average decrease in their formation energies when compared to the crystalline phase, which may have important implications for the possible presence of vacancies in the HfO_2 region when compared to the interfacial SiO_2 layer. This indicates that it will be very important to investigate oxygen vacancies in the amorphous $Hf_{1-x}Si_xO_2$. We also find that there is an increase in the number of fourcoordinated Si atoms in the amorphous $Hf_{1-x}Si_xO_2$ as x increases, which may help to explain the different behaviors of phase separation in these systems for distinct Si contents.[24,26]

We acknowledge support from the Brazilian Agencies FAPESP (Grants No. 2005/54190-9 and No. 2005/59581-6) and CNPq, and the CENAPAD-SP for computer time.

*wlscopel@if.uff.br

[1] J. Robertson, Eur. Phys. J.: Appl. Phys. **28**, 265 (2004).

[2] P. W. Peacock, K. Xiong, K. Y. Tse, and J. Robertson, Phys. Rev. B **73**, 075328 (2006); K. Xiong, Y. Du, K. Tse, and J. Robertson, J. Appl. Phys. **101**, 024101 (2007); S. Monaghan, J. C. Greer, and S. D. Elliott, Phys. Rev. B **75**, 245304 (2007), and references therein.

[3] A. Kerber, E. Cartier, L. Pantisano, R. Degraeve, T. Kauerauf, Y. Kim, A. Hou, G. Groeseneken, H. E. Maes, and U. Schwalke, IEEE Electron Device Lett. **24**, 87 (2003).

[4] S. Zafar, A. Kumar, E. Gusev, and E. Cartier, IEEE Trans. Device Mater. Reliab. **5**, 45 (2005).

[5] K. Tse, D. Liu, K. Xiong, and J. Robertson, Microelectron. Eng. **84**, 2028 (2007).

[6] P. Broqvist and A. Pasquarello, Appl. Phys. Lett. **89**, 262904 (2006).

[7] Y.-S. Lin, R. Puthenkovilakam, and J. P. Chang, Appl. Phys. Lett. **81**, 2041 (2002).

[8] S. Zafar, E. Cartier, and E. P. Gusev, Appl. Phys. Lett. **80**, 2749 (2002).

[9] B. K. Park, J. Park, M. Cho, C. S. Hwang, K. Oh, Y. Han, and D. Y. Yang, Appl. Phys. Lett. **80**, 2368 (2002).

[10] D. Ceresoli and D. Vanderbilt, Phys. Rev. B **74**, 125108 (2006).

[11] P. Broqvist and A. Pasquarello, Microelectron. Eng. **84**, 2416 (2007).

[12] C. Kaneta and T. Yamasaki, Microelectron. Eng. **84**, 2370 (2007).

[13] The AIMD simulations were performed by using ultrasoft pseudopotentials (Ref. 14) and a GGA approximation for the exchange-correlation potential (Ref. 15), as implemented in the VASP code (Ref. 16). In order to generate an atomic structure of amorphous HfO_2, we have used a 96 atom supercell (32 Hf and 64 O), obtained as a $(2\times2\times2)$ expansion of the 12 atom monoclinic unit cell. The plane wave energy cutoff was 400 eV, and the Brillouin zone was sampled at the Γ point. During the simulations, the size of supercell was kept constant at the optimized bulk crystal value. The simulation started from the crystalline structure at room temperature, and the system was gradually heated during 1000 MD to 5500 K (time step of 3×10^{-15} s), and was then equilibrated at this average temperature (NVE ensemble) for 2000 MD steps, and subsequently cooled from 5500 K down to 300 K in 1000 MD steps, and equilibrated for another 500 MD steps. As a final procedure, the structure was fully relaxed ($T=0$ K) such that in the equilibrium final geometry of the disordered system the forces on all the atoms were smaller than 0.025 eV/Å.

[14] D. Vanderbilt, Phys. Rev. B **41**, 7892 (1990).

[15] J. P. Perdew, J. A. Chevary, S. H. Vosko, K. A. Jackson, M. R. Pederson, D. J. Singh, and C. Fiolhais, Phys. Rev. B **46**, 6671 (1992).

[16] G. Kresse and J. Hafner, Phys. Rev. B **47**, 558 (1993); G. Kresse and J. Hafner, *ibid.* **48**, 13115 (1993); G. Kresse and J. Furthmuller, Comput. Mater. Sci. **6**, 15 (1996).

[17] X. Y. Zhao, D. Ceresoli, and D. Vanderbilt, Phys. Rev. B **71**, 085107 (2005).

[18] T. V. Perevalov, V. A. Gritsenko, S. B. Erenburg, A. M. Badalyan, H. Wong, and C. W. Kim, J. Appl. Phys. **101**, 053704 (2007).

[19] A. Zupan, P. Blaha, K. Schwarz, and J. P. Perdew, Phys. Rev. B **58**, 11266 (1998).

[20] J. Kang, E.-C. Lee, and K. J. Chang, Phys. Rev. B **68**, 054106 (2003).

[21] W. L. Scopel, A. J. R. Silva, W. Orellana, and A. Fazzio, Appl. Phys. Lett. **84**, 1492 (2004).

[22] A. S. Foster, F. Lopez Gejo, A. L. Shluger, and R. M. Nieminen, Phys. Rev. B **65**, 174117 (2002).

[23] M. Houssaa, L. Pantisanoa, L.-Å. Ragnarssona, R. Degraevea, T. Schrama, G. Pourtoisa, S. De Gendta, G. Groesenekena, and M. M. Heyns, Mater. Sci. Eng., R. **51**, 37 (2006).

[24] S. Monaghan, J. C. Greer, and S. D. Elliott, J. Appl. Phys. **97**, 114911 (2005).

[25] D. Fischer and A. Kersch, Microelectron. Eng. **84**, 2039 (2007).

[26] S. Stemmer, Z. Chen, C. G. Levi, P. S. Lysaght, B. Foran, J. A. Gisby, and J. R. Taylor, Jpn. J. Appl. Phys., Part 1 **42**, 3593 (2003); S. Stemmer, Y. Li, B. Foran, P. S. Lysaght, S. K. Streiffer, P. Fuoss, and S. Seifert, Appl. Phys. Lett. **85**, 3143 (2003).